18th World IMACS / MODSIM Congress, Cairns, Australia 13-17 July 2009
http://mssanz.org.au/modsim09

Propagation of wind and slope backfires

Rossa, C.G. and Viegas, D.X.

Associação para o Desenvolvimento da Aerodinâmica Industrial (ADAI), Department of Mechanical Engineering, University of Coimbra, 3030 Coimbra, Portugal
Email: xavier.viegas@dem.uc.pt

Abstract: When studying and/or modelling fire behaviour, in the great majority of cases, research is focused on the head fire, i.e. on fire spreading either upslope or with favourable wind, the influence of favourable wind on fire behaviour being the most studied parameter. This is understandable as the prediction of the fire section that spreads with favourable wind or slope is of great practical interest in many aspects particularly in fire fighting management. For this reason the majority of fire behaviour simulators like Behave and the Canadian Forest Fire Behaviour Prediction System deal mainly with head or flank fires. In these simulators it is generally assumed that backfires spread at a practically constant rate of spread and that the fire contour of a backing fire is well represented by a half circle or ellipse. Yet, backing fires are of practical interest as well because they can represent large sections of the fire perimeter and their behaviour is dependent on local convection conditions.

To our knowledge few studies were made with the purpose of studying backfire propagation i.e. fire spreading downslope or with contrary wind. One example of backfire behaviour analysis is the work of Weise and Biging (1997) where laboratory experiments analysing both downslope and contrary wind propagation are performed, comparing the results against four prediction models, for a maximum wind velocity of -1.1 m/s and for a maximum slope of -17º.

In the present paper ROS results from 30 laboratory experiments of fire spreading downslope for slopes varying from 0º to -60º, and from 12 experiments of fire spreading with contrary wind for wind up to -4.5 m/s, are presented. The fuels used were straw and *Pinus pinaster* dead needles and the most important parameters influencing fire spread, like fuel moisture, fuel load and fuel bed bulk density, among others were carefully monitored.

An analysis of the fire line evolution with time using infra-red images, was made, showing the existence of convective effects that cause the fire to have a dynamic behaviour, i.e. the fire changes its spread properties over time even for constant boundary conditions. A mathematical model is proposed and based on the laboratory experiments the necessary parameters to its application are determined.

Keywords: *forest fire behaviour modelling, downslope propagation, contrary wind propagation, dynamic fire behaviour, convective effects.*

1. INTRODUCTION

Backfires are usually neglected when modelling forest fire behaviour although they represent a large percentage of the fire line extension and their study permits a better understanding of some particular features of this type of fires and of fire behaviour in general. Reviewing previous work on fire behaviour we can find many studies on slope head fires (e.g. Van Wagner, 1968; Rothermel, 1972) and many more on wind headfires (e.g. Pagni and Peterson, 1973; Albini, 1981; Viegas and Neto, 1991). For example Van Wagner (1968) studied fire behaviour, for wind and slope headfires and some slope backfires, in red pine using field and laboratory experiments. In the laboratory experiments he varied slope from 0º to 35º. The well known Rothermel's (1972) model, that incorporates wind and slope effects, does not consider backfires and in the Behave fire simulator (Andrews *et al.*, 2003) the ROS for backfires is considered constant.

On the other hand not much attention has been given either to slope backfires (e.g. Van Wagner, 1988; Lyons and Weber, 1993) or wind backfires (e.g. Van Wagner, 1968). Van Wagner (1988) presents results from 22 laboratory experiments of fires spreading downslope concluding that the ROS decreases from 0º to around -25º, increasing again up to -45º where it attained a value equal to level ground. Weise and Biging (1997) analysed slope and wind headfires and backfires, performing 65 laboratory experiments where they varied wind up to 1.1 m/s and slope up to 17º, each for heading and backing fires.

The present work aims to contribute to a better understanding of backfires. Using two large scale test rigs, described in the next section, and a smaller one, under controlled burning conditions, wind and slope backfires are performed and analysed. The experiments are made in a wide range of possible slope angles and wind velocities, monitoring the fire ROS and recording visible and infra-red images from a top view and visible images from the side view. The effects of slope and wind on the ROS are analysed and using the infra-red images the fire line evolution is assessed. The results are used to develop an algorithm for predicting the fire line evolution based on simple equations and the parameters necessary to the algorithm application are also determined and presented.

2. METHODOLOGY

2.1. Fire line evolution related concepts

In the experimental tests presented here, in order to be able to compare ROS results between experiments in a more accurate way we shall consider a non-dimensional ROS, R', that is given by $R'=R/R_0$, where R is the ROS measured during the experiment under wind or slope effect and R_0 is the basic ROS, i.e. the ROS for the same conditions of fuel moisture, and fuel bed properties, but with no wind or slope. In this way we obtain a non dimensional rate of spread that represents the influence of wind or slope as a ratio of the fire rate of spread on a horizontal terrain without ambient wind.

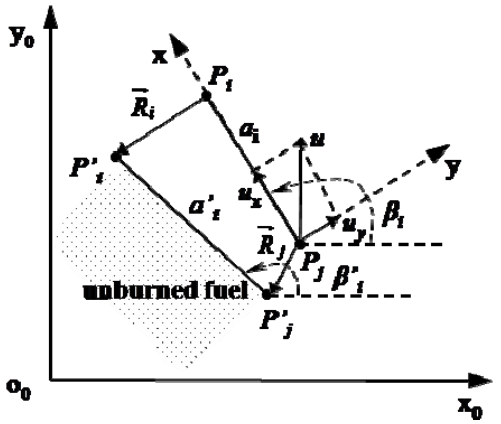

Figure 1 – Fire line segment S_i length, a_i and angle, β_i, evolution from one given time instant to another and decomposition of the wind velocity vector in its parallel and perpendicular components to a fire line element.

In order to analyse the fire line shape evolution we will consider that it can be represented by a given number, n, of straight segments. If we consider a given segment S_i with length a_i and inclination β_i, in the fire line in the general case it will have a movement composed by a translation, an extension, and a rotation (Fig. 1). The translation and extension result from the fire spread, given that due to the combustion reaction in each time instant fuel ahead of the fire line is being ignited and at the same time in the combustion zone the flame progressively extinguishes as the burning fuel runs out causing the fire to move in space and the fire line to extend its perimeter. On the other hand the rotation results from the existence of convection along the fire line which causes that a given point will have an energetic state different from another point either upwards or downwards. For that reason the points will have different ROS and if we consider that they define a segment it will change its angle during a given time interval (Fig. 1). We define the segment angular velocity by Eq. (4).

The heat transport along the fire line can be easily understood if we decompose the wind velocity (Fig. 1b), $\vec{u}$, in its parallel and perpendicular components to the ROS direction, u_y and u_x, respectively, and that can be obtained using Eq. (2) and (3), being the component u_x the responsible for the heat transport. We consider that the characteristic flow velocity, $\vec{u}$, is applicable both to a wind and to a slope driven fire, because the combustion reaction causes air entrainment, i.e. an induced air flow, that has an effect that is similar to

ambient wind. In fact, as referred in Eq. (1), during fire spread the local flow velocity is given by the sum of the ambient wind, $\vec{u}_0$, if it exists or an equivalent flow velocity associated to slope, and the induced velocity, $\vec{u}_i$. The induced air flow is usually variable over time and is the responsible for the fire's dynamic behaviour, i.e. the change of its spread properties even for constant boundary conditions (Viegas, 2004).

$$\vec{u} = \vec{u}_0 + \vec{u}_i \tag{1}$$

$$u_x = |\vec{u}|.\sin\beta \tag{2}$$

$$u_y = -|\vec{u}|.\cos\beta \tag{3}$$

$$\omega = \frac{d\beta}{dt} \tag{4}$$

2.2. Experimental procedures

Test rigs: In order to assess the ROS and fire line shape evolution of backfires spreading under the effect of slope or wind a series of tests were conducted in the Laboratory of Forest Fire Research of the University of Coimbra, located in Lousã. A total of 42 tests, 21 for each of the 2 different fuel beds used, were carried out in 3 different test rigs that are described below.

The test rigs were the Canyon Table DE4, Combustion Table DE1, and the Combustion Tunnel TC2. Except for the Combustion Table DE1, where only the ROS was analysed, in the other 2 test rigs both the ROS and fire line evolution were assessed. The Canyon Table DE4 has two symmetrical faces of 6×4 (L×W) m^2 each, driven hydraulically and can be positioned as a single slope or as a canyon with geometrical angles varying in the range $0º < \alpha < 40º$. In this study only the slope configuration was used forming a fuel bed of $2.5×3m^2$ on one face of the table and 8 experiments were made for variable slope. The Combustion Table DE1 has a burn area of $1.4×1.5\ m^2$, and can be tilted manually and positioned with geometrical angles varying in the range $0º < \alpha < 65º$. The total burn area was used and 22 experiments were made. The Combustion Tunnel TC2 has a useful area of $9×3m^2$ but the fuel bed in the present experiments had an area of $2.5×2\ m^2$. The reference wind velocity above the fuel bed can be varied continuously between 0 and 5 m/s. Twelve experiments were made for variable wind.

Fuel beds: Two types of fine fuel particles were used in the present study: dry straw and *Pinus pinaster* dead needles. Fuel load, fuel homogeneity and fuel bed bulk density were controlled and maintained constant during the experiments. On the contrary as fuel moisture content was not conditioned so it had to be monitored carefully during the preparation and before each experiment, although its value was always in the range $11\% < m_f < 13\%$.

All tests were prepared according to a previously defined protocol adopted in our Laboratory for this type of experiments (Rossa, 2008). The fuel load used in the present tests was $0.6\ kg/m^2$ (dry basis) and fuel moisture content was measured before each test. Strings were stretched over the fuel bed at a constant spacing in order to determine ROS by registering the time instant at which each string was broken by the advancing fire. Three strings were used in the TC2 with spacing of 0.5m, and in the DE1 and DE4 test rigs six strings were used with spacing of 0.1 m and 0.25 m respectively. In the DE4 and TC2 experiments the ignition was placed along a 0.8 m line parallel to the wind or slope gradient direction at the centre of the fuel bed width. In the DE1 experiments ignition was made perpendicular to the slope gradient direction and the first half of the fuel bed was used to determine the backfire ROS and the second half to determine the basic rate of spread, R_o, after tilting the rig back to α=0º. For the remaining experiments R_o was determined using a separate fuel bed with the same overall properties as the main one but with a smaller area of approximately $1x1m^2$. In a group of experiments in a test table for a given fuel, each experiment in the series was performed in a random order to avoid any bias in the results.

Data processing: The ROS was evaluated from the slope of a straight line fitted to the distance versus time measurements made with the strings. The fire line evolution, on the other hand, required an infrared image analysis in order to obtain the fire line evolution contours. This process will be briefly described below.

For each experiment after selecting the frames to analyse, using CAD software, the contours of the fire line for each frame were drawn and corrected to represent orthogonal projections of the fire contours to a plane parallel to the camera lens. In the initial line, at $t=t_o$, we chose n points that define $n-1$ segments of the fire line. An example is shown in Fig. 2 for test DE4-03. Segments from the right and left sides of the fire perimeter were referred as S_{iR}, S_{iL} respectively. The centreline element was referred as S_{CL}. Our results did

not exhibit any difference between the two sides and therefore the analysis was made for the entire set of data. At each point P_i the tangent direction to the fire line contour is determined by geometric construction; from this a perpendicular line is drawn to define the ROS direction and to determine the point P'_i corresponding to the position of point P_i at time $t'=t+\Delta t$. This process was repeated for each time step and the coordinates x_i, y_i of each point were determined using the CAD software and were then used to determine the various parameters used in this study. The time step Δt used for straw and pine fuel bed tests was respectively 20s and 60s.

3. RESULTS AND DISCUSSION

3.1. Rate of spread

The results for the non-dimensional ROS, R', for backfires on a slope are shown in Fig. 3a. The first group of experiments performed in the test rig DE4, which aimed to analyse both the ROS and also the fire line shape, includes a total of 8 tests, 4 using straw and 4 using pine needles, in a range of slopes varying from -40º<α< -10º with 10º intervals. Regarding the ROS results, for both fuels, it appeared that R' had a value slightly lower than 1, but more or less constant over the range of tested slopes. However, in order to study backfire propagation for a wider range of slopes (up to -60º) a new group of experiments was planned. It was decided to use an angle interval $\Delta\alpha$=5º and given the high number of experiments to perform (a total of 22 experiments, 11 for each fuel) a smaller test rig was used (table DE1) and only ROS results were assessed.

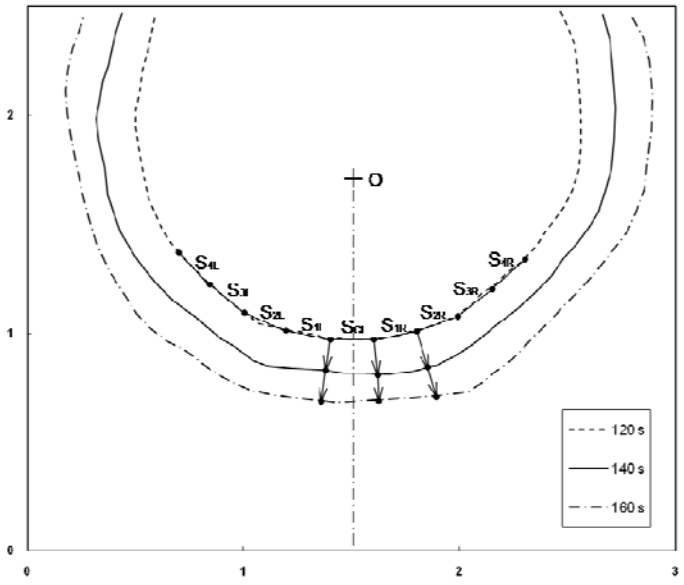

Figure 2 – Example of fire line partition in segments and their evolution from one time instant to another for test DE4-03 (α=-30º; Fuel: straw; Fuel load: 0.6 kg/m^2).

Although the test rig DE1 allowed for angles up to -65º it was verified that for α<-45º for pine needles and α<-55º for straw, spotting started to occur due to falling embers, first inside the fuel bed depth and afterwards also outside it. For this reason the results obtained for angles out of the referred range are not presented.

Looking at the results in Fig. 3, one is tempted to conclude that for backfires spreading in both fuels the value of R' is constant but a more careful analysis shows that the backfire velocity has an oscillatory evolution over the range of analysed slopes. It is interesting to notice that the oscillation pattern is similar for both fuels. This can be easily observed if in the graphic shown in Fig. 3a we translate the points relative to the backfire propagation velocity in pine needles by 10º to the left, i.e. the velocity that actually corresponds to -5º would correspond to -15º and there forth. Doing this we can see that the ROS values are very similar but also that their minimum and maximum values occur with the exact same interval for both fuels.

In order to estimate the relative error of the measurements we analysed the cases for which we had repetitions with the same slope and fuel although tests were performed either in DE1 or DE4. The maximum difference on the values of R' for straw and for pine needles was respectively 18% and 12%. The amplitude of the oscillation of R' values for different slope angles in the range -40º<α<-25º for straw (ST-DE1) and for pine needles (PN-Trans) was respectively 18% and 51%. This means that the amplitude of oscillation for straw is of the same order of the maximum estimated relative deviation in the estimation of R', but for pine needles the oscillation is over four times that difference. Considering that the results are obtained from single test burns, that each experiment in the data series was performed in a random order to avoid any bias and that the oscillation pattern is similar for both fuels we have a good indication that it should not be a consequence of variance in the measurements.

Although in the case of wind backfires (Fig. 3b) this oscillatory behaviour is not so clear, it appears to follow a similar pattern. Since higher wind velocities cannot be used, because fire spread is not sustained, to better

understand the ROS evolution over the possible range of wind velocities, further tests must be performed for wind velocities in between those already used.

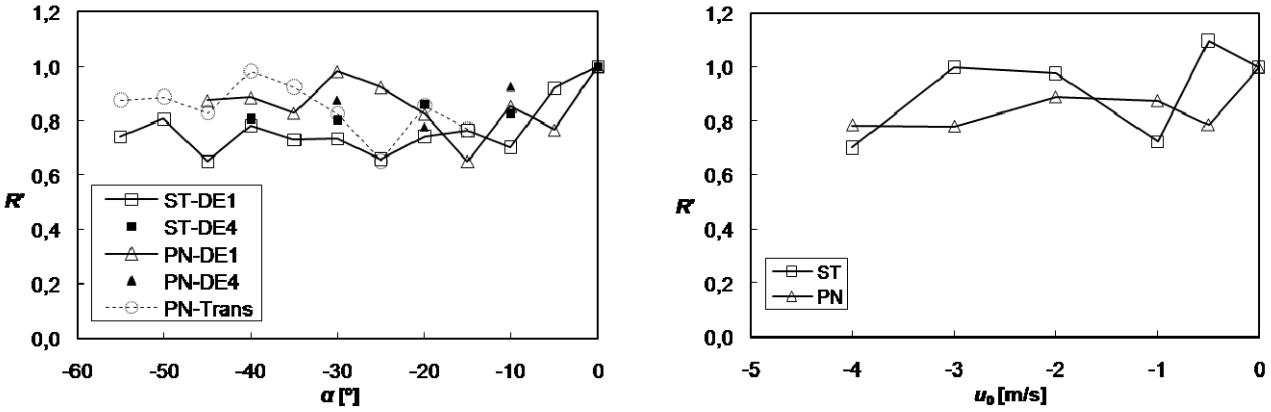

(a) (b)

Figure 3 – Non-dimensional rate of spread results from single test burns for *Pinus pinaster* dead needles and straw, fuel load of 0.6 kg/m^2: (a) for variable slope. The dotted line corresponds to a translation of the data for pine needles with a displacement of 15º; (b) for variable wind velocity.

Figure 4 – Flame geometry for tests with variable slope from 0º≤α≤40º. The variation of the flame length and flame angle for different slope angles can be observed (Fuel: straw; Fuel load: 0.6 kg/m^2).

A possible explanation for this oscillation of the fire ROS is the balance of heat transfer by radiation and convection at the fire line. Radiation is greatly dependent on flame geometry, namely its inclination angle and length, that are influenced by the local flow properties: as we tilt the table the air entrainment increases causing the enhancement of the combustion reaction and of the buoyancy forces which cause the flame to become more vertical, but the increase of the air velocity also forces the flame to tilt backwards. The balance between these two effects seems to produce an oscillatory evolution of the ROS with decreasing slope or flow velocity. Pictures of the flame geometry for backfires with different slope angle are shown in Fig. 4 to support this assumption. Comparing the flame for horizontal spread and -10º we can see that the later, although not very different in length, is more tilted backwards. The reduction in the view factor between the flame and the fuel bed causes a decrease in the heat transfer by radiation and therefore a decrease in the ROS, which corresponds to a local minimum in the graphic (Fig. 3a). When comparing the flame for -20º with the one for -10º we can see that the first has a slightly smaller tilt backwards but a significantly higher flame length, which allows for an increase of the transferred radiation and explaining the increase in the ROS. For -25º when compared with -20º, we can see both an increase in the flame tilt backwards and a decrease in the flame length which causes a new decrease in the ROS and justifies another local minimum in the graphic.

Then for -35º and -40º, when compared with -25º, respectively, we can see first an increase in the flame length and a very similar tilt, and afterwards a decrease in the backwards tilt, which explains the successive increase in the ROS. It must be said that the behaviour that is illustrated in these pictures was consistent in each test and for each configuration the properties that were described above were practically the same for the duration of the test.

3.2. Fire line extension

During its evolution a segment of the fire line will change its length. We can define a relative extension of the fire line element ε_a according to Eq. (5).

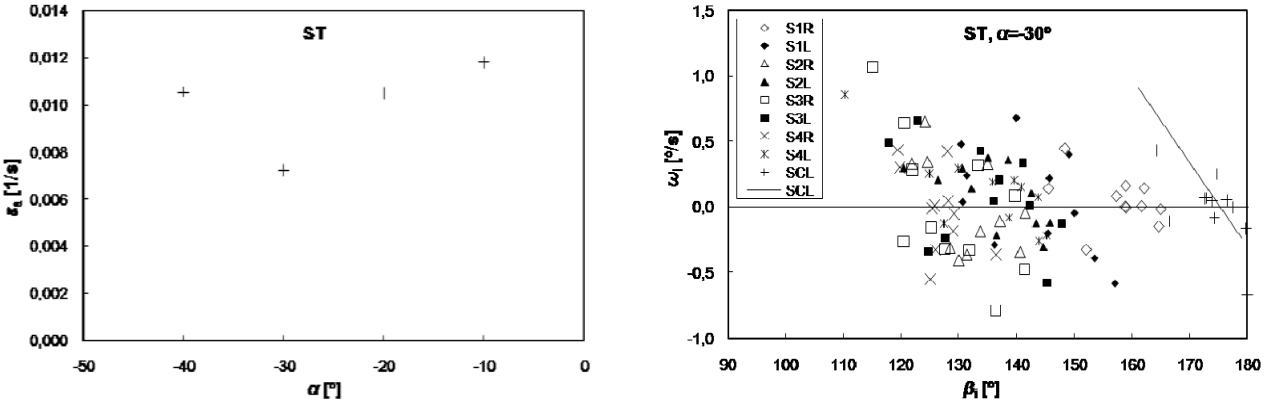

(a) (b)

Figure 5 – Results for straw, fuel load of 0.6 kg/m^2, Δt=20s: (a) average relative extension of the segments as a function of the slope angle; (b) angular velocity of the segments as a function of its initial angle, α=-30º.

Analysing the data obtained in our tests we concluded that it is reasonable to consider that this parameter is constant for a given fuel and slope angle or wind velocity. We therefore computed the average values of ε_a for each case. The results of ε_a obtained for straw as a function of α are shown in Fig. 5a. The results obtained for the other cases are quite similar and also exhibit a minimum for α=-30º.

$$\frac{1}{a_{\mathrm{i}}} \cdot \frac{da_{\mathrm{i}}}{dt} = \varepsilon_a \tag{5}$$

$$a'_{\mathrm{i}} = a_{\mathrm{i}} + \varepsilon_a \cdot a_{\mathrm{i}} \cdot \Delta t \tag{6}$$

3.3. Fire line rotation

In Fig. 5b we can see the angular velocity plotted as a function of the segment angle in a given time instant, for a backfire on a slope of α=-30º for straw. This type of behaviour was observed in all slope and wind backfires for both fuels. Taking Fig. 5b as an example we can adjust a straight line given by Eq. (9) to each set of points corresponding to a given segment. It was found that the slope, m_r, of the various trendlines was more or less constant, for each fuel, for all segments and for all tested slopes. This means that the segments rotation in backwards spreading fires seems to depend essentially on the fuel bed properties. For that reason the value of m_r for each fuel was considered to be the average of the obtained values for each segment for each tested slope. The same procedure was done for the wind results and the corresponding parameters are presented in Table 1.

Table 1. Parameters obtained by fitting for the prediction of the segments rotation for straw and pine needles (Fuel load: 0.6 kg/m^2).

Parameter	Slope backfires		Wind backfires	
	ST	PN	ST	PN
m_r	-6.40×10^{-2}	-2.4×10^{-2}	-6.2×10^{-2}	-3.30×10^{-2}
m_β	7.77×10^{-1}	7.72×10^{-1}	9.33×10^{-1}	7.07×10^{-2}
b_β	35.38	27.91	11.80	44.47

Using Eq. (7) and (8) we can predict a fire line segment angle evolution along time. Because each segment has a different angle, that corresponds to a zero angular velocity, β_{int}, the value of b_r must be determined for each case. Since β_{int} has a good relation with the segment angle at the beginning

of each experiment, β_{ini}, and again depends essentially on the fuel bed properties, we could determine the parameters of Eq. (9) by a linear regression after plotting β_{int} against β_{ini} for a given fuel, for the range of tested slopes or wind velocities. The correlation coefficient r^2 was always above 0.77. The determined parameters are presented in Table 1. Using Eq. (10) we can easily determine b_r for a given segment. In Fig. 5b we can see the fitting obtained for the set of points associated to a particular segment S_{CL} of the fire line.

$$\omega_i = m_r \cdot \beta_i + b_{r,i} \tag{7}$$

$$\beta_i' = \beta_i + \omega_i \cdot \Delta t \tag{8}$$

$$\beta_{\text{int},i} = m_\beta \cdot \beta_{ini,i} + b_\beta \tag{9}$$

$$b_{r,i} = -m_r \cdot \beta_{\text{int},i} \tag{10}$$

4. CONCLUSION

Results from laboratory experiments of backfires spreading on a slope ($-60º < \alpha < 0º$) and in a wind ($0 < u < -4.5$ m/s), using straw and pine needles fuel beds are presented. An analysis was made to backfires ROS and to the fire line evolution shape and a simple model to predict fire line evolution was developed. Further work is being done in order to integrate the present algorithm with a previous model (Viegas, 2002; Viegas *et al.*, 2006) to predict of the entire fire line evolution of a point ignition in a wind or slope induced fire.

ACKNOWLEDGMENTS

The collaboration given to the experimental program that supports this paper by Miss Telma Domingues is gratefully acknowledged. The support given by the *Fundação para a Ciência e a Tecnologia*, under project *CODINF*, (Contract POCTI/EME/341128/00) to this study is also gratefully acknowledged. The first author performed this study with the support given by the *Fundação para a Ciência e a Tecnologia*, under the Fellowship ref. SFRH/BD/17669/2004.

REFERENCES

Albini, F.A. (1981) A model for the wind-blown flame from a line fire. *Comb. Flame*, **43**. 155-174.

Andrews, P.L., Bevins, C.D., Seli, R.C. (2003) BehavePlus fire modeling system, version2.0: User's Guide. Gen. Tech. Rep. RMRS-GTR-106WWW. Ogden, UT: USDA Forest Service. 132pp.

Lyons, P.R. and Weber, R.O. (1993) Geometrical effects on flame spread rate for wildland fine fuels. *Comb. Sci. Tech.*, **89**, 153-165.

Pagni, P.J., and Peterson, T.G. (1973) Flame spread through porous fuel. 14th Symposium on Combustion. The Combustion Institute. Pittsburgh, 1099-1107.

Rossa, C.G. (2008) Protocol for the experiments made in LEIF during the firefighter training for the National Firefighter School by the CEIF team. Internal technical report *(in Portuguese)*, Center of Studies on Forest Fires (CEIF), ADAI, Coimbra, 18 pp.

Rothermel, R.C. (1972) A mathematical model for predicting fire spread in wildland fuels. USDA Forest Service. Intermountain Forest and Range Experiment Station, Ogden, Utah. Res. Paper INT-115. 40 pp.

Van Wagner, C.E. (1968) Fire behaviour mechanisms in a red pine plantation: field and laboratory evidence. Forestry Branch Departmental Publication No. 1229. Ottawa. 30 pp.

Van Wagner, C.E. (1988) Effect of slope on fires spreading downhill. *Can. J. For. Res.*, **18**, 818-820.

Viegas, D.X., and Neto, L. P. (1991) Wall shear-stress as a parameter to correlate the rate of spread of a wind induced forest fire. *Int. J. Wildland Fire*, **1 (3)**, 177-188.

Viegas, D.X. (2002) Fire line rotation as a mechanism for fire spread on a uniform slope. *Int. J. Wildland Fire*, **11**, 11-23.

Viegas, D.X. (2004) On the existence of a steady-state regime for slope and wind driven fire. *Int. J. Wildland Fire*, **13 (1)**, 101-117.

Viegas, D.X., Rossa, C.G., Oliveras, I., and Piñol, J. (2006) Fireline Rotation Model. In: Proceedings of the V ICFFR. 27-30 November 2006, Figueira da Foz.

Weise, D.R. and Biging, G.S. (1997) A qualitative comparison of fire spread models incorporating wind and slope effects. *Forest Sci.*, **43(2)**, 170-180.